Interband Phase Modes and Nonequilibrium Soliton Structures in Two-Gap Superconductors

A. Gurevich[1] and V. M. Vinokur[2]

[1]*Applied Superconductivity Center, University of Wisconsin, Madison, Wisconsin 53706*
[2]*Materials Science Division, Argonne National Laboratory, Argonne, Illinois 60439*

We predict a new dynamic state in current-carrying superconductors with a multicomponent order parameter. If the current density J exceeds a critical value J_t, an interband breakdown caused by charge imbalance of nonequilibrium quasiparticles occurs. For $J > J_t$, the electric field penetrating from current leads gives rise to various static and dynamic soliton phase textures, and voltage oscillations similar to the nonstationary Josephson effect. We propose experiments to observe these effects which would probe the multicomponent nature of the superconducting order parameter.

There are experimental and theoretical evidences that several superconductors, including MgB_2 [1,2], $NbSe_2$ [3], the heavy-fermion UPt_3 [4], and organic $(TMTSF)_2X$ [5] and κ-BEDT [6], as well as the superfluid ^{3}He-A [7] may have a multicomponent order parameter ψ with internal degrees of freedom [7,8]. For two weakly coupled s-wave order parameters $\psi_1 = \Delta_1 e^{i\theta_1}$ and $\psi_2 = \Delta_2 e^{i\theta_2}$ on different disconnected parts of the Fermi surface (as in MgB_2), the internal degree of freedom is the interband phase difference $\theta(\mathbf{r}, t) = \theta_1 - \theta_2$. In this case, in addition to the phase-locked states ($\theta = 0, \pi$), peculiar phase textures $\theta(\mathbf{r}, t)$ can occur. Soft modes associated with fluctuations of $\theta(\mathbf{r}, t)$ are nearly decoupled from gap fluctuations and behave like the Anderson plasmons in Josephson junctions [7]. These modes may manifest themselves as additional resonances in the ac Josephson effect [9], or static 2π kinks in $\theta(x)$ [10].

In this Letter, we show that the interband phase mode does not contribute to the static magnetic response, but becomes crucial for *nonequilibrium* current states in which the charge imbalance at normal leads results in phase slip structures $\theta(\mathbf{r}, t)$ propagating into a superconductor (Fig. 1). We predict a new dynamic state above the critical current density $J > J_t$ which marks the onset of the current-induced breakdown of the superconducting state. For the multicomponent ψ, such breakdown is a two-stage process. First, at $J = J_t$, an interband breakdown occurs, resulting in spontaneous dislocationlike textures in $\theta(x, t)$, and ac voltage oscillations at fixed gaps $\Delta_{1,2}$. The second stage corresponds to higher J close to the depairing current density $J_d > J_t$, at which both gaps $\Delta_{1,2}$ get suppressed by the pair breaking effects (for weak interband coupling, $J_t \ll J_d$).

We derive the equations of motion for θ and the electric field $\mathbf{E}$ near the critical temperature $T \approx T_c$, using the time-dependent Ginzburg-Landau (TDGL) equations [11] generalized to a two-gap superconductor:

$$2\Gamma_\mu(\partial_t - 2\pi ci\varphi/\phi_0)\psi_\mu = -\delta F/\delta\psi_\mu^*. \qquad (1)$$

Here μ runs from 1 to 2, φ is the electric potential, ϕ_0 is the flux quantum, c is the speed of light, Γ_μ are damping constants, and the free energy $F = \int d^3\mathbf{r}(f_1 + f_2 + f_m + f_{\text{int}})$ contains the magnetic part $f_m = |\nabla \times \mathbf{A}|^2/8\pi$, the GL intraband part f_μ, and the interband interaction f_{int},

$$f_\mu = \alpha_\mu|\psi_\mu|^2 + \frac{\beta_\mu}{2}|\psi_\mu|^4 + g_\mu \left|\left(\nabla + \frac{2\pi i}{\phi_0}\mathbf{A}\right)\psi_\mu\right|^2, \qquad (2)$$

$$f_{\text{int}} = \gamma(\psi_1\psi_2^* + \psi_1^*\psi_2) = 2\gamma\Delta_1\Delta_2\cos\theta, \qquad (3)$$

where $\mathbf{A}$ is the vector potential, α, β, and g are the GL expansion coefficients, γ is the interband coupling
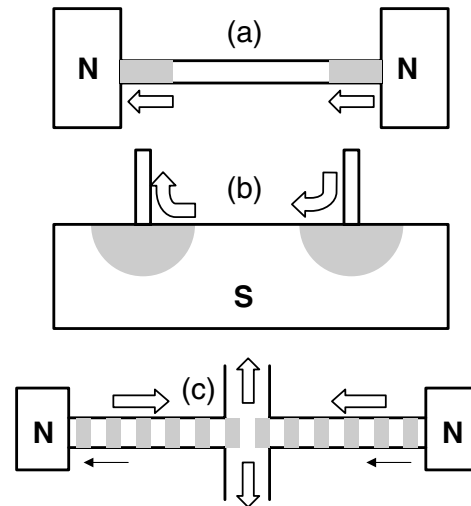

FIG. 1. Geometries in which the interband phase breakdown could occur. Here N labels normal electrodes, gray domains show phase solitons moving along thin arrows, and block arrows indicate current directions. Static phase textures form in microbridges (a) and point contacts (b), while in the 4-terminal geometry (c) the solitons and antisolitons continuously annihilate in the center.

constant, and the asterisk means complex conjugation. The qualitative results of this work remain valid for any periodic dependence $f_{int}(\theta)$, so the simplest form of f_{int} disregarding gradient terms [12] is taken. We consider weak interband coupling $\gamma \ll \alpha_{1,2}$ [13,14], which is likely the case in MgB_2 [1,2].

The imaginary part of Eq. (1) gives

$$\Gamma_\mu\left(\dot{\theta}_\mu - \frac{2\pi c}{\phi_0}\varphi\right)\Delta_\mu^2 = -\frac{2\pi g_\mu}{\phi_0}\nabla(\Delta_\mu^2\mathbf{Q}_\mu) \pm \gamma\Delta_1\Delta_2\sin\theta, \quad (4)$$

$$\nabla \times \nabla \times \mathbf{A} = (4\pi/c)(\sigma\mathbf{E} + \mathbf{J}_s), \quad (5)$$

where $\theta = \theta_1 - \theta_2$, $\mathbf{Q}_\mu = \mathbf{A} + \phi_0\nabla\theta_\mu/2\pi$, the plus sign corresponds to $\mu = 1$, $\sigma\mathbf{E}$ is the Ohmic current density proportional to the electric field $\mathbf{E} = -\nabla\varphi - \dot{\mathbf{A}}/c$ and the normal conductivity σ, and the supercurrent

$$\mathbf{J}_s = -8\pi^2 c(g_1\Delta_1^2\mathbf{Q}_1 + g_2\Delta_2^2\mathbf{Q}_2)/\phi_0^2 \quad (6)$$

is a sum of independent intraband contributions. The usual boundary conditions, $(i\partial_n + 2\pi A_n/\phi_0)\psi_\mu = i\psi_\mu/l_\mu$, between a superconductor and a normal metal ensure zero perpendicular J_s for *both* ψ_1 and ψ_2.

If $\gamma \ll \alpha_{1,2}$, the gaps Δ_μ are decoupled from θ, so static equations (4) and (5) yield the London equation for **H**, and the sine-Gordon equation $L_\theta^2\nabla^2\theta = \text{sgn}(\gamma)\sin\theta$ for θ [10]. The latter has a single-soliton or staircase solutions similar to the vortex solutions in long Josephson contacts [15]. However, the physics of these θ solitons is different from that of the Josephson vortices. Indeed, the Josephson vortices reduce the Gibbs free energy in a magnetic field $H > H_{c1}$ because they carry the quantized magnetic flux and are driven by the Lorentz force of supercurrents. By contrast, θ solitons do not carry magnetic flux and thus do not interact with supercurrents, but can be driven by a nonequilibrium *charge density* injected from normal electrodes. As a result, equilibrium nonuniform solutions $\theta(x)$ are energetically unfavorable as compared to the phase-locked state $\theta = 0$ (for $\gamma < 0$) or π (for $\gamma > 0$), however various dynamic or quenched phase textures can be generated during current-induced interband breakdown.

To describe the evolution of these phase textures, we obtain the equation of motion for θ, expressing $\mathbf{Q}_{1,2}$ in Eqs. (4) in terms of **J** and $\nabla\theta$, and then subtracting the equations for θ_1 and θ_2 from each other. This yields

$$\tau_\theta\dot{\theta} = L_\theta^2\nabla^2\theta \mp \sin\theta + \alpha_\theta\text{div}\mathbf{J}_s, \quad (7)$$

where the relaxation time τ_θ, the decay length L_θ, and the charge coupling parameter α_θ are given by

$$\tau_\theta = \Gamma_1\Gamma_2\Delta_1\Delta_2/|\gamma|(\Gamma_1\Delta_1^2 + \Gamma_2\Delta_2^2), \quad (8)$$

$$L_\theta^2 = g_1g_2\Delta_1\Delta_2/|\gamma|(g_1\Delta_1^2 + g_2\Delta_2^2), \quad (9)$$

$$\alpha_\theta = \frac{\phi_0\Delta_1\Delta_2(\Gamma_1 g_2 - \Gamma_2 g_1)}{4\pi c|\gamma|(g_1\Delta_1^2 + g_2\Delta_2^2)(\Gamma_1\Delta_1^2 + \Gamma_2\Delta_2^2)}. \quad (10)$$

The signs in Eq. (7) correspond to the sign of γ. As follows from Eq. (7), the θ mode does not contribute to the static magnetic response, since $\text{div}\mathbf{J}_s = 0$ for any distribution of bulk supercurrents. However, the θ mode interacts with a nonuniform electric field due to non-equilibrium charge imbalance, $\text{div}\mathbf{J}_s = -\sigma\text{div}\mathbf{E}$ near the normal leads. It is the difference in the injected intra-band charge densities, which provides the driving term in Eq. (8) because of the band asymmetry, $\Gamma_1 g_2 \neq \Gamma_2 g_1$.

To obtain the equation for **E**, we add Eqs. (4) for θ_1 and θ_2, then take the gradient of the sum and express $\mathbf{Q}_{1,2}$ in terms of **J** and $\nabla\theta$. This yields

$$\tau_e\dot{\mathbf{E}} + \mathbf{E} - L_e^2\text{grad div}\mathbf{E} + \alpha_e\nabla\dot{\theta} = \tau_e\dot{\mathbf{J}}/\sigma, \quad (11)$$

where $\mathbf{J}(t)$ is the driving current density, L_e is the electric field penetration depth, τ_e is the charging time constant, and the coupling term $\alpha_e\nabla\dot{\theta}$ describes an electric field caused by moving phase textures:

$$\tau_e = \sigma\phi_0^2/8\pi^2 c^2(g_1\Delta_1^2 + g_2\Delta_2^2), \quad (12)$$

$$L_e^2 = \sigma\phi_0^2/8\pi^2 c^2(\Gamma_1\Delta_1^2 + \Gamma_2\Delta_2^2), \quad (13)$$

$$\alpha_e = 2|\gamma|\Delta_1\Delta_2\alpha_\theta. \quad (14)$$

Equations (7) and (11) describe nonlinear electrodynamics of a two-gap superconductor at fixed $\Delta_{1,2}$. We use these equations to calculate $\theta(x,t)$ in a current-carrying microbridge of length $2a$ [Fig. 1(a)]. Below the critical current density J_t the bridge is in a phase-locked state, except localized phase kinks at the edges (Fig. 2). For $J > J_t$, the interband breakdown causes penetration of phase textures in the bulk, as shown in Figs. 3 and 4. Here J_t can be calculated from the static Eq. (7) ($\gamma < 0$):

$$L_\theta^2\theta'' - \sin\theta + \alpha_\theta J_s' = 0, \quad (15)$$

where $\theta'(\pm a) = J_s(\pm a) = 0$, $\theta'(0) = 0$, and the prime denotes differentiation over x.

We first obtain J_t for a long ($a \gg L_\theta \gg L_e$) bridge where $J_s'(x)$ is essential only in a narrow region $a - L_e < x < a$ of the electric field penetration. Then the static equation $\alpha_\theta J = 2L_\theta|\sin\theta(a)/2|$, for the maximum value of $\theta(a)$ at the edge has solutions only if $J < J_t$, where

$$J_t = 2L_\theta/\alpha_\theta. \quad (16)$$

In the opposite limit $L_\theta \ll L_e$, the static solutions $E(x) = E_0\cosh(x/L_e)/\cosh(a/L_e)$, $\sin\theta(x) = -\sigma\alpha_\theta E'(x)$, exist only if $\sigma\alpha_\theta E'(a) < 1$ or $J < J_t$. Here E_0 is the electric field in the normal lead, and

$$J_t = L_e/\alpha_\theta\tanh(a/L_e). \quad (17)$$

For $\Gamma_1 = \Gamma_2$, $g_1 \gg g_2$, $\alpha_1 \sim \alpha_2$, and $\Delta_1 \sim \Delta_2$, Eq. (16) gives $J_t \sim (\gamma g_2/\alpha g_1)^{1/2}J_d \ll J_d$. The ratio g_2/g_1 can be
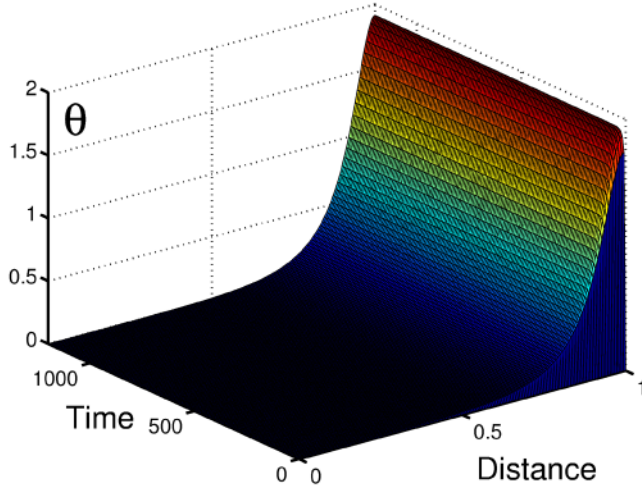
FIG. 2 (color online).   Formation of a static phase soliton in $\theta(x)$ near the bridge edge after the current density was instantaneously turned on from 0 to $J = 0.99 J_t$ at $t = 0$. Times and distances from the center ($x = 0$) are taken in the units of τ_θ and a, respectively, $L_e = a/10$, $L_\theta = 0.1 L_e$.

further reduced by nonmagnetic impurities, for example, by Mg vacancies in MgB_2, which mostly cause scattering in the π band (band 2 in our notations).

For $J > J_t$, the charge-induced interband breakdown gives rise to striking dynamic states in which θ solitons periodically appear near the current leads and then propagate into the bulk. We solved Eqs. (7)–(14) numerically in the limit $\alpha_e \alpha_\theta \ll \min(\tau_\theta L_e^2, \tau_e L_\theta^2)$ of weak coupling between θ and E, for which div$\mathbf{E}$ in Eq. (7) is mostly determined by the *static* $E(x)$, while the last term in Eq. (14) gives a small ac correction to E of the second order in α_e [16]. Figure 2 shows the evolution of $\theta(x, t)$ near the current lead in a microbridge [Fig. 1(a)] as

J was instantaneously turned on from zero to a value below J_t. Such current step eventually produces a stable distribution $\theta(x)$ localized near the edge, while the bulk of the bridge remains in the phase-locked state. For $J < J_t$, this behavior is characteristic of all geometries in Fig. 1, for which the dynamics of $\theta(x, t)$ for $J > J_t$ can be very different.

We start with the bridge [Fig. 1(a)], for which current flow does not change direction, so $E(x, t)$ and $\theta(x, t)$ are even and odd functions of x, respectively, $E(\pm a, t) = E_0$, $E'(0, t) = 0$, $\theta(0) = 0$, $\theta'(\pm a, t) = 0$, and supercurrents in both bands vanish at the normal electrodes, where $J = \sigma E$. In this case θ solitons first appear at the bridge edges, but for $J > J_t$, they are pushed to the bulk by the strong gradient of $E(x)$. Then the next soliton forms near the edge and the process repeats periodically, resulting in the propagation of two soliton chains from the opposite current leads as shown in Fig. 3. After the first two solitons in the chains collide in the center they stop, while new solitons keep entering the bridge. During this soliton pileup, the mean slope $\bar{\theta}'(t)$ increases, reaching a critical value $\bar{\theta}'_c \simeq \alpha_\theta J/L_\theta^2$ (for $J \gg J_t$) at which the soliton generation at the edges stops and a static texture forms. The excess dc resistance of the bridge for $J > J_t$ remains the same as for $J < J_t$, however, during the soliton penetration, $t < t_c \sim \tau_\theta a \bar{\theta}'_c / 2\pi$, a transient resistance and voltage oscillations are generated. A similar behavior occurs at the point contact [Fig. 1(b)], in which concentric soliton shells propagate into the bulk.

A very different kind of soliton dynamics occurs in the 4-terminal geometry [Fig. 1(c)], for which currents flow in the opposite directions, making 90° turns around the central stagnation point ($x = 0$) where $\nabla\theta = 0$ by symmetry. In this case $E(x)$ is an odd function of x so the driving charge density div$\mathbf{E}$ does not change sign along
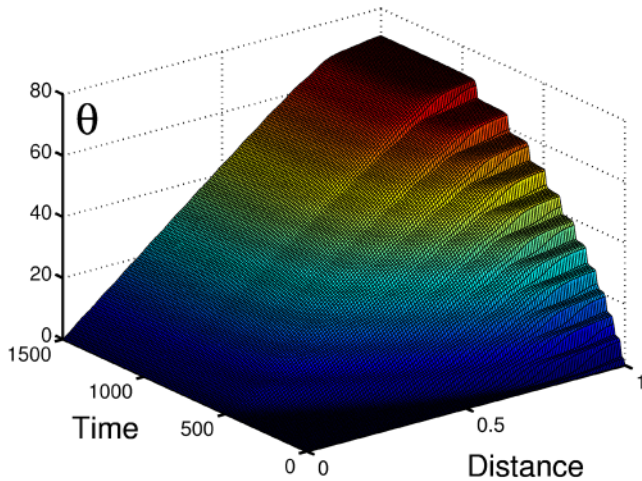

FIG. 3 (color online).   Dynamics of formation of a static soliton chain in the bridge of length $2a$ after $J(t)$ was instantaneously turned on from 0 to $1.025 J_t$ at $t = 0$. Only the right half ($0 < x < a$) is shown, and the rest is the same as in Fig. 2.
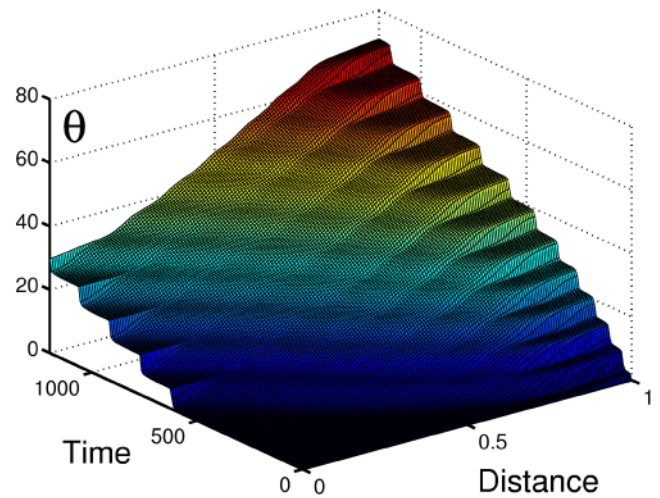

FIG. 4 (color online).   Moving soliton shuttle along the right half of the horizontal leg ($0 < x < a$) in the 4-terminal geometry shown in Fig. 1(c). $J(t)$ was instantaneously turned on from 0 to $1.012 J_t$ at $t = 0$, and the rest is the same as in Fig. 2.

the horizontal leg of the cross in Fig. 1(c); the total charge along the horizontal leg is compensated by the opposite charge distributed along the vertical leg. The asymmetry of $E(x)$ causes generation of solitons and antisolitons with θ shifted by π at the opposite current leads, which then move toward the center of the cross where they annihilate, as shown in Fig. 4. Such continuous soliton motion takes place if the width w_y of the vertical leg is greater than the width w_x of the horizontal leg, so that the current density in the horizontal leg I/w_x exceeds J_t, while the vertical leg remains in the phase-locked state $I/w_y < J_t$, where I is the total sheet current. If the lengths of the strips are much greater than L_e, the soliton-antisoliton annihilation is unaffected by the charge imbalance near the current leads.

Two different dynamic states represented in Figs. 3 and 4 have clear analogs in the theory of long Josephson contacts. Namely the transient soliton penetration in the bridge in Fig. 3 is analogous to vortex penetration in a long Josephson junction in a magnetic field $H > H_{c1}$, since in both cases the driving terms (charge and magnetization current densities, respectively) are asymmetric functions of x. By contrast, the soliton dynamics in the 4-terminal geometry is analogous to the steady-state annihilation of self-field Josephson vortices and antivortices in a long Josephson junction with a transport current. Because the total charge along the horizontal strip in Fig. 1(c) is nonzero, all θ solitons are pushed in the same direction (antisolitons move in the opposite direction), similar to the flux flow of the Josephson vortices driven by the Lorentz force of the transport current.

For $J > J_t$, the soliton shuttle in Fig. 4 results in voltage oscillations on the bridge. For $L_e \gg L_\theta$, the ac voltage $V_\omega(t) = \sum_{m=1}^{\infty} V_m \cos(m\omega t + \psi_m)$ between the points $x_1 \sim a/2$ and $x_2 = a$ can be estimated by integrating Eq. (11): $\tau_e \dot{V}_\omega + V_\omega = \alpha_e[\dot{\theta}(x_1, t) - \dot{\theta}(x_2, t)]$. The oscillating part of $\dot{\theta}_s = \dot{\theta}(x_2, t) - \dot{\theta}(x_1, t)$ obeys the equation $\tau_\theta \dot{\theta}_s + \sin\theta_s = \beta$, for which $\tau_\theta \dot{\theta}_s = 2\sqrt{\beta^2 - 1} \sum_{m=1}^{\infty} (\beta - \sqrt{\beta^2 - 1})^m \cos m\omega t$, $\beta = J/J_t$, and $\omega = \tau_\theta^{-1}\sqrt{\beta^2 - 1}$ [17]. Hence, $\tan\psi_m = m\omega\tau_e$, and

$$V_m \simeq \frac{2\alpha_e}{\tau_\theta}\sqrt{\beta^2 - 1}\frac{(\beta - \sqrt{\beta^2 - 1})^m}{\sqrt{1 + (m\omega\tau_e)^2}}. \qquad (18)$$

Here $V_m(\beta)$ is maximum at $\beta = \beta_m$, where $\beta_m \simeq 1 + 0.5(\tau_\theta/m\tau_e)^{2/3}$, and $V_m(\beta_m) \simeq 2\alpha_e/m\tau_e$ for $\tau_\theta \ll \tau_e$. The effects considered in this work are due to interband tunneling [7], so the generation of θ solitons does not require any weak links. Unlike the Josephson vortex, a single θ soliton moving with a constant velocity v does not carry magnetic flux, thus it does not cause any total dc voltage V, as follows from Eq. (11) integrated over x: $V = \alpha_e v \int_{-\infty}^{\infty} \theta'' dx = 0$. However, the phase slippage near the normal lead increases the electric field penetration depth $\tilde{L}_e$. For $J \gg J_t$, substitution of $\tau_\theta \dot{\theta} = -\alpha_\theta E'/\sigma$ from Eq. (8) into Eq. (11) yields $\tilde{L}_e^2 = L_e^2 +$

$\alpha_e\alpha_\theta/\sigma\tau_\theta$. This effect increases the excess dc sheet resistance of the strip by $R_{ex} = (\tilde{L}_e - L_e)/\sigma w$.

The soft interband θ mode could also manifest itself in rf absorption at frequencies below the small gap Δ_2, depending on the polarization of the rf electric field $\mathbf{E}$. If $\mathbf{E}(t)$ is parallel to the sample surface, then $\text{div}\mathbf{E} = 0$, so the phase mode is not excited by the rf field. However, the θ mode contributes to the rf impedance if the rf field has a component perpendicular to the sample surface.

In conclusion, we predict an interband breakdown induced by nonequilibrium quasiparticles in two-gap superconductors. It results in spontaneous generation of static and/or dynamic phase textures, causing voltage oscillations and excess dc resistance. The observation of these effects would unambiguously indicate the multicomponent nature of the superconducting order parameter.

[1] A. Liu, I. I. Mazin, and J. Kortus, Phys. Rev. Lett. **87**, 087005 (2001); H. J. Choi *et al.*, Nature (London) **418**, 758 (2002).
[2] G. Karapetrov *et al.*, Phys. Rev. Lett. **86**, 4374 (2001); F. Giubileo *et al.*, *ibid.* **87**, 177008 (2001); H. Schmidt *et al.*, *ibid.* **88**, 127002 (2002).
[3] T. Yokoya *et al.*, Science **294**, 2518 (2001).
[4] R. Joynt and L. Tallifer, Rev. Mod. Phys. **74**, 235 (2002).
[5] D. Jerome and H. J. Schulz, Adv. Phys. **51**, 293 (2002).
[6] J. Singleton and C. Mielke, Contemp. Phys. **43**, 63 (2002).
[7] A. J. Legget, Prog. Theor. Phys. **36**, 901 (1966); Rev. Mod. Phys. **47**, 331 (1975).
[8] M. Sigrist and K. Ueda, Rev. Mod. Phys. **63**, 239 (1991).
[9] D. F. Agterberg, E. Demler, and B. Janko, Phys. Rev. B **66**, 214507 (2002).
[10] Y. Tanaka, Phys. Rev. Lett. **88**, 017002 (2002).
[11] N. Kopnin, *Theory of Nonequilibrium Superconductivity* (Oxford University Press, New York, 2001).
[12] H. Doh *et al.*, Phys. Rev. Lett. **83**, 5350 (1999).
[13] H. Suhl, B. T. Matthias, and L. R. Walker, Phys. Rev. Lett. **3**, 552 (1959).
[14] For $\alpha_2, \gamma \gg \alpha_1$, the induced gap $\Delta_2 = \gamma\Delta_1 \cos\theta/\alpha_2$ depends on θ. In that case θ is a poor variable, because Eq. (1) turns into a single TDGL equation for Δ_1 with $\alpha_1 \to \alpha_1 - \gamma^2 \cos^2\theta/\alpha_2$, which describes only locked states with $\theta = 0$ or π.
[15] A. Barone and G. Paterno, *Physics and Applications of the Josephson Effect* (Wiley, New York, 1982).
[16] For $\tau_e \gg \tau_\theta$ and $L_e^2 \gg L_\theta^2$, the ac component of E obeys $\tau_e \dot{E} = L_e^2 E'' + \alpha_e \dot{\theta}'$, whence $E' \simeq -\alpha_e \dot{\theta}/L_e^2$ for small soliton velocities $v \ll L_e/\tau_e$, and $E' \simeq \alpha_e \theta''/\tau_e$ for $v \gg L_e/\tau_e$. This E' just renormalizes the length and time scales in Eq. (7): $\tau_\theta \to \tau_\theta + \alpha_e\alpha_\theta/L_e^2$, $L_\theta \to L_\theta$ for $v \ll L_e/\tau_e$, and $\tau_\theta \to \tau_\theta$, $L_\theta^2 \to L_\theta^2 + \alpha_e\alpha_\theta/\tau_\theta$ for $v \gg L_e/\tau_e$, but does not change the behavior of $\theta(x, t)$.
[17] L. G. Aslamazov and A. I. Larkin, JETP Lett. **9**, 87 (1969).